






Received : 13.05.2019 & Accepted : 24.06.2019 & Published (online) : 26.06.2019

Designing, Dynamic Modeling and Simulation of ISTECCOPTER

Sezer Coban^{1*} , Hasan Hüseyin Bilgiç² , Tugrul Oktay³ 

¹ College of Aviation, Iskenderun Technical University, Iskenderun/Hatay

² Iskenderun Technical University, Faculty of Engineering and Natural Sciences, Iskenderun/Hatay

³ Department of Aeronautical Engineering, Erciyes University, Kayseri

Abstract

In this study, ISTECCOPTER was modeled, performance evaluations were made and control system was designed. ISTECCOPTER is a four-rotor Unmanned Aerial Vehicle (UAV) consisting of the abbreviation of Iskenderun Technical University and the combination of the words copter. For the control system, lateral, longitudinal and vertical take-off of the UAV (Unmanned Aerial Vehicle) and the separate mathematical model of the descent operations were extracted and expressed as the state space model. The mathematical model of the wind distortions that will affect the aircraft during the flight was created and the situation was added to the space model. Proportional Integral Derivative (PID) control algorithm was used as a control. The unmanned aircraft was modeled in Solidworks and the simulations in Matlab / Simulink program. the ISTECCOPTER is planned to have 4 brushless DC motors and has a weight of approximately 1.5 kg without load and 1 kg of payload is planned.

Keywords: PID, simulink, UAV(unmanned aerial vehicle).

1. Introduction

The main components to be used in ISTECCOPTER; The body, APM flight control card, brushless DC motor, propeller, electronic speed controller (ESC), load holding mechanism, GPS, telemetry, RC (Radio Controlled) transmitter and

receiver are LiPo batteries. During the design, the rotating vane ISTECCOPTER will be able to go autonomously to the coordinates given in advance, to load and release autonomously in these positions and to 'failsafe mode ot to be activated in possible

* Corresponding Author: Dr. Sezer ÇOBAN sezer.coban@iste.edu.tr



This is an open access article distributed under the terms of the Creative Commons Attribution 4.0 International Licence

Citation : Çoban S., Bilgiç H.H., Oktay T. (2019). Designing, dynamic modeling and simulation of ISTECCOPTER . Journal of Aviation, 3 (1), 38-44. DOI: 10.30518/jav.564376

signal interruptions. Thanks to the data from the ISTECONPTER (telemetry and radio receiver and transmitter), the data will be read in real time. In this task to be performed manually, according to the rules appropriate to the requirements of the task will be acted. The logic of the desired algorithm in autonomous task is briefly as follows; The water bottles in different weights in one area are taken from the field respectively, weighing the weight, finding the desired area according to this weight and leaving the bottle. The software to be used for this task will be provided with the Arduino-based programming language. At this point, it will be ensured that the electronic components required for the task will work together with the generated circuit diagrams and software codes.

ISTECONPTER has 4 brushless DC motors and it is planned to have a load of approximately 1.5 kg without load and carry 1 kg of useful cargo. The technical picture of ISTECONPTER shown in Figure 1. shall be 620,85 mm, including the propellers, and 194,06 mm in height and its body shall be manufactured with 3D printer from PLA material. According to this information, CAD and isometric views of the technical parameters required for ISTECONPTER, which are designed and manufactured according to this information, are given in Figure 1 and Figure 2 respectively.

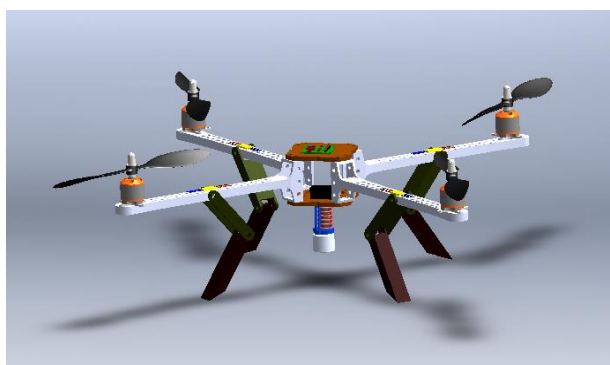


Figure 1. ISTECONPTER's CAD design

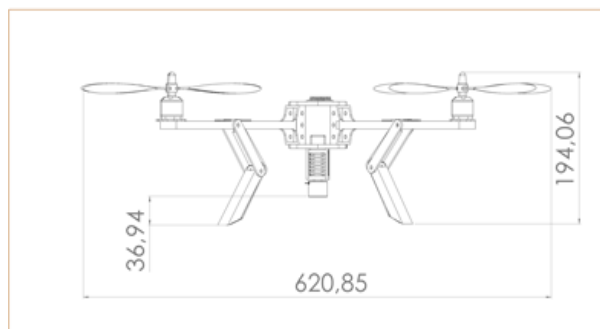


Figure 2. ISTECONPTER Technical Drawing (Front View)

In order to realize the first task in a shorter time by saving weight, our revolving winged UAV is designed with 4 motors. The first task will be done manually. In order to carry out the second task, the electromagnet-controlled load-bearing mechanism shown in Figure 3 will be added and the UAV will be autonomous. An alternative to the retention mechanism is a retention system. In addition, a telemetry system will be added to the ground station for real-time monitoring of the flight to be used in all missions.



Figure 3. ISTECONPTER electromagnet controlled load holding mechanism

2. ISTECONPTER Mathematical Model

The yaw motion is obtained from the counter torque between each of the propellers. While each rotor rotates at an equal angular velocities, the net yaw is zero, but the speeds difference between the two pairs creates a positive or negative yaw. Forward or backward movement which is related to the pitch angle can be obtained by increasing the back rotor thrust and decreasing the front rotor thrust. Finally, a sideways motion which is related to the roll, ϕ angle can be achieved by increasing the

left rotor thrust and decreasing the right rotor thrust. Figure 4 shows the various motions of a istecopter due to changes in rotor speeds.

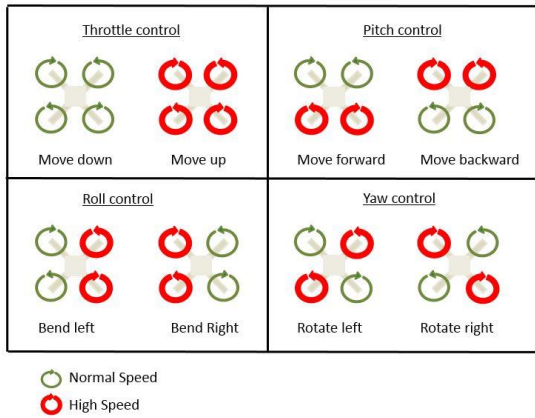


Figure 4. ISTECOPTER motions

The dynamic model of istecopter is obtained from Newton–Euler approach. Here, the Newton–Euler approach is used with the following assumptions [1]: the structure is rigid and symmetric, the propellers are rigid, the thrust and the drag are proportional to the square of speed, ground effect is neglected. If the velocities of the propellers are expressed by f_i , the total thrust generated by the four propellers is defined by FM as follows:

$$F_M = [0 \quad 0 \quad \sum_{i=1}^4 f_i] \quad (1)$$

Where f_i [2]

$$f_i = 4.392399 \times 10^{-8} \cdot \text{RPM} \cdot \frac{d^{3.5}}{\sqrt{\text{pitch}}} (4.23333 \times 10^{-4} \cdot \text{RPM} \cdot \text{pitch} - V_0) \quad (2)$$

RPM is propeller rotations per minute; pitch is propeller pitch, in inches; d is propeller diameter, in inches; and V_0 is the forward airspeed, freestream velocity, or inflow velocity (depending on what you want to call it), in m/s.

The inputs must apply to the system in order to control the behavior of the istecopter. The torque applied to the device along an axis is the difference between the torques applied by each propeller on the other axes [3]. The values of the input forces and torques proportional to the squared speeds of the rotors[4],

$$\left. \begin{aligned} f_t &= U_1 = b(\Omega_1^2 + \Omega_2^2 + \Omega_3^2 + \Omega_4^2) \\ \tau_x &= U_2 = bl(\Omega_3^2 - \Omega_1^2) \end{aligned} \right\}$$

$$\left. \begin{aligned} \tau_y &= U_3 = bl(\Omega_4^2 - \Omega_2^2) \\ \tau_z &= U_4 = d(\Omega_2^2 + \Omega_4^2 - \Omega_1^2 - \Omega_3^2) \end{aligned} \right\} \quad (3)$$

Where l the distance between any rotor and the center of the istecopter, b is the thrust factor and d is the drag factor. The full istecopter non-linear dynamic model with the x,y,z motions as a consequence of a pitch, roll and rotation is as follows.

$$\begin{aligned} \dot{x} &= w[s(\phi) c(\psi) + c(\phi) c(\psi) s(\theta)] - v[c(\phi) s(\psi) - c(\psi) s(\phi) s(\theta) + u[c(\psi) c(\theta)]] \\ \dot{y} &= v[c(\phi) c(\psi) + s(\phi) s(\psi) s(\theta)] - w[c(\psi) s(\phi) - c(\phi) s(\psi) s(\theta) + u[c(\theta) s(\psi)]] \\ \dot{z} &= w[c(\phi) c(\theta)] - u[s(\theta)] + v[c(\theta) s(\phi)] \\ \dot{\phi} &= p + r[c(\phi) t(\theta)] + q[s(\phi) t(\theta)] \\ \dot{\theta} &= q[c(\phi)] - r[s(\phi)] \\ \dot{\psi} &= r \frac{s(\phi)}{c(\theta)} + q \frac{s(\phi)}{c(\theta)} \\ \dot{u} &= (vr - wq) + g s(\theta) \\ \dot{v} &= (wp - ur) - g c(\theta) s(\phi) \\ \dot{w} &= (uq - vp) - g c(\theta) s(\phi) \frac{U_1}{m} \\ \dot{p} &= \frac{I_y - I_z}{I_x} qr + \frac{U_2}{I_x} \\ \dot{q} &= \frac{I_z - I_x}{I_y} pr + \frac{U_3}{I_y} \\ \dot{r} &= \frac{I_x - I_y}{I_z} pq + \frac{U_4}{I_z} \end{aligned} \quad (4)$$

3. Flight Control System

In the case of Matlab / Simulink, the state space model of our unmanned aerial vehicle was removed before real time flight. Simulation model (state-space model) and P, I, D coefficients were used to maximize autonomous performance (rise time, sitting time and maximum time) before real-time flight applications. In addition, the data obtained from the unmanned aerial vehicle to be produced in real time and the autopilot to be supplied is examined experimentally. Defining the dynamic modeling of the aircraft is important in developing control systems. High accuracy models have a great impact on the quality of designed control algorithms.

PID is a control mechanism used in common industrial control systems. It is also widely used in istecopter control. A PID controller calculates the difference between a set point and a desired set point in the process as an "error" value. The controller tries to reach the set point by downloading the minimum value of the error.

The control output is passed through three separate mathematical operations and is obtained by summing. System effects are as follows.

Proportional Effect (P): Effective as the output multiplied by a certain "gain" value of the error. Calculates the current error.

Integral Effect (I): The effect of the control is proportional to the sum of all the errors in the moment up to the moment the effect is calculated. In other words, the integral effect means the sum of errors the system has made in the past.

Derivative Effect (D): It has a proportional effect on the output of the system, according to the change of the error. So it calculates the prediction of the future error. 65% of the applications in the industry have PID applied. Karl Arstom defines this algorithm which has a wide application area as follows:

$$u(t) = K_p e(t) + K_i \int_0^t e(v)dv + K_d \frac{de(t)}{dt} \quad (5)$$

Where, K_p proportional coefficient, K_i integral coefficient and K_d is the derivative coefficient.

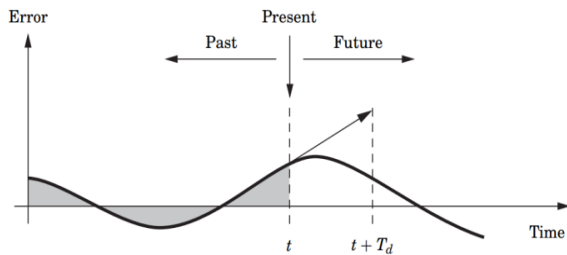


Figure 5. A PID controller takes control action based on past, present, and future

If a traditional PID structure is represented by blocks, it is as follows:

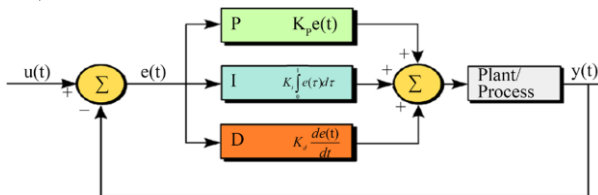


Figure 6. Traditional PID controller

The PID control has two disadvantages [5]:

- 1) Because the derivative effect is accounted for using the system's error signal, it can cause the system to move away from the linear region.
- 2) The integral effect must be limited to the minimum and maximum values as it takes time to change the integral sign.

Figure 7 used a new approach to prevent undesirable situations [6].

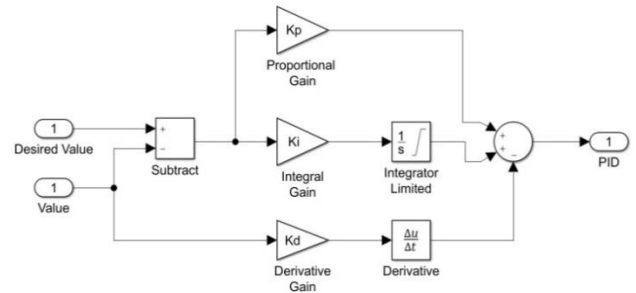


Figure 7. PID new approach

The flight control card has been selected as arduino-based autonomous flight and the ardupilot flight control card (Figure 8) was selected. APM Planner 2.0 has been selected for open source earth station software. The ground station will provide the connection with the telemetry system.

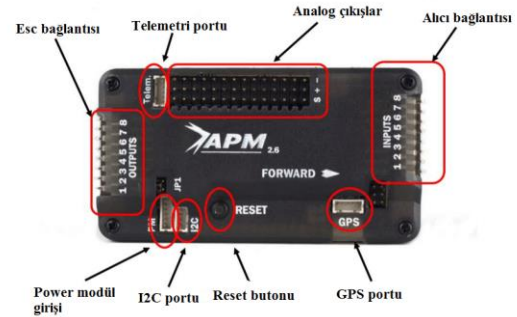


Figure 8. APM flight control card

We used an adjustable autopilot using flight observations and our autopilot system has a classic autopilot structure. There are three layers for the hierarchical control structure and are divided into outer loop, middle loop and inner loop which was showed in figure 9 .

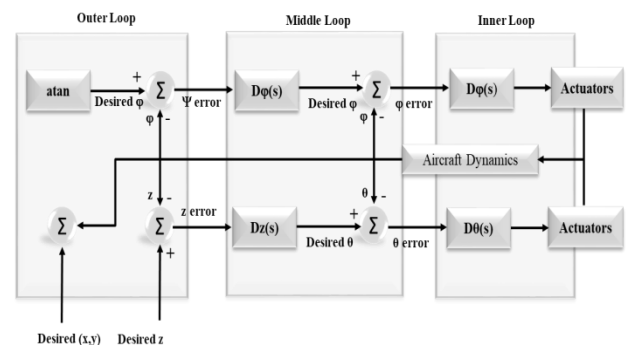


Figure 9. Control structure of autopilot system

Accordingly, the longitudinal, lateral flight and hover PID blocks are as follows:

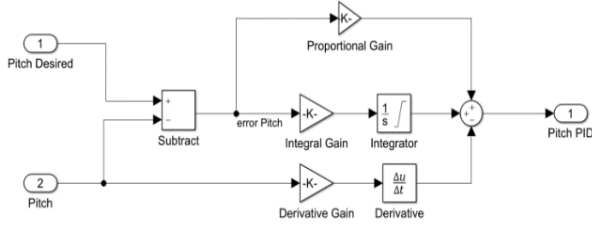


Figure 10. longitudinal flight PID block [7]

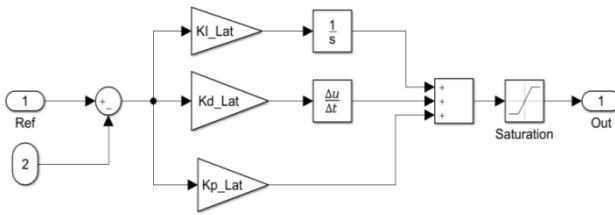


Figure 11. lateral flight PID block [7]

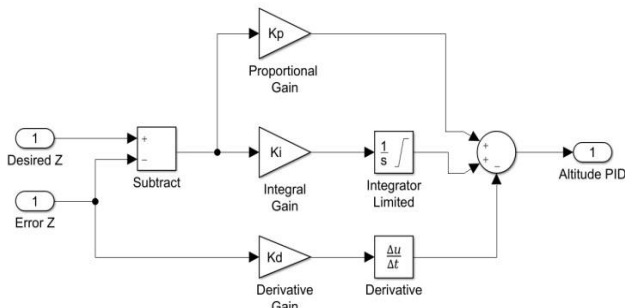


Figure 12. Hover Flight PID Block [8]

In order to integrate the components that we will use, the necessary circuit diagram is made in the olup Fritzing 'program and the parts included in the program are combined as electronic circuit diagram as shown in figure 13.

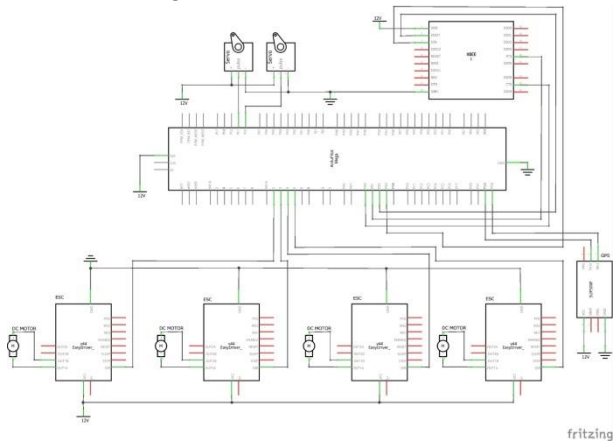


Figure 13. Electronic Circuit Diagram

UAVs missions in real-life applications encounter significant disturbances generated by atmospheric turbulence, which is a complex physical phenomenon and is typically modeled using elements from stochastic fluid theory. Therefore, it is preferable to pass a white noise through a forming filter in order to generate a proper wind-gust model. In literature, two main forming filters can be found: the Dryden and the von Karman. It is von Karman approach that is utilized in this paper [9].

4. Results and Discussion

Depending on the model and parameters istecopter longitudinal, hover and lateral flight simulink models are as follows.

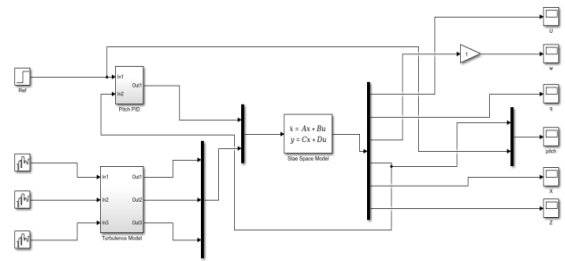


Figure 14. Longitudinal Flight Simulink Model

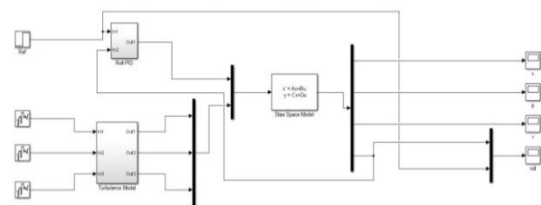


Figure 15. Lateral Flight Simulink Model

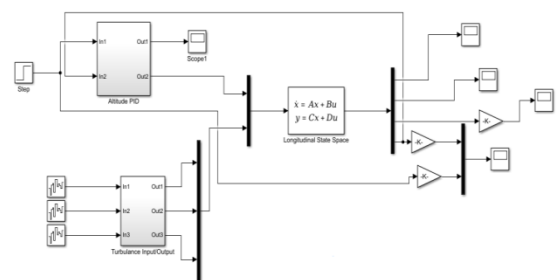


Figure 16. Hover Flight Simulink Model

The state space models created for each flight mode were entered into the state space model in the simulink separately. In addition, to test that istecopter works in a disturbances environment, the

Von Karman Model has been added to the simulation.

The following graphs are obtained for each flight mode according to the simulation results.

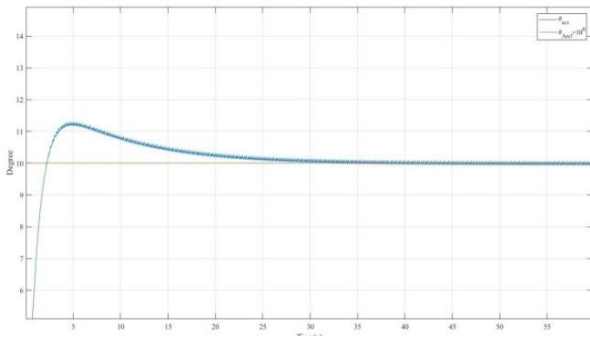


Figure 17. Pitch Angle

Figure 17 illustrates the closed-loop responses of some longitudinal state variables and the closed-loop response of the elevator surface with longitudinal movement in the longitudinal motion 5-degree pitch angle tracking and tracking. It is seen that the ISTECCOPTER longitudinal autopilot system has successfully followed the desired trajectory, and also other condition variables and control surface did not show excessive behavior.

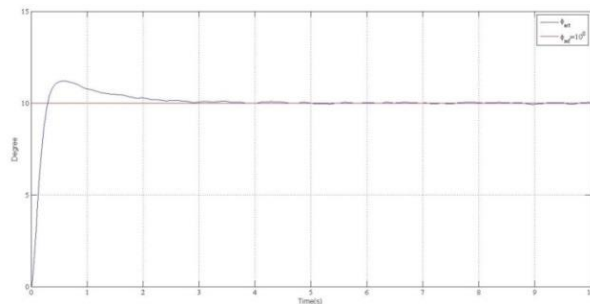


Figure 18. Roll Angle

Figure 18 illustrates the closed-loop responses of some lateral state variables and the closed-loop response of the aileron surface associated with lateral movement during the trajectory tracking of 5 degrees in lateral motion and trajectory tracking. It is evident that the lateral autopilot system successfully follows the desired trajectory, and also other condition variables and the control surface did not show excessive behavior.

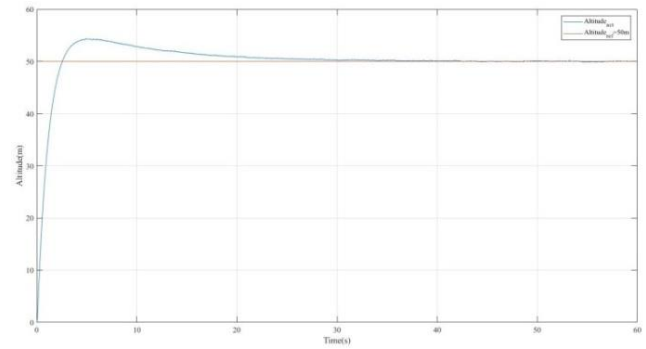


Figure 29: Yaw Angle

Figure 18 illustrates the closed-loop responses of some vertical state variables and the closed-loop response of the rudder surface associated with vertical motion during the trajectory tracking of 5 degrees in vertical motion and trajectory tracking.

5. Conclusions

In this study, longitudinal, lateral and hover flight of ISTECCOPTER is discussed. Isteccopter model was created in Solidworks program and data obtained from it was made with Simulink model. During longitudinal, lateral and hover flight, rise time, overshoot, settling time, steady state error which is criteria for design performances were obtained within satisfactory borders. During longitudinal, lateral and hover flight, demanded circle was controlled successfully. During longitudinal, lateral and hover flight, saturation function on the control surface obeyed successfully. During longitudinal, lateral and hover flight, other state variables did not demonstrate catastrophic behavior [10].

The PID algorithm was used to control the isteccopter. The von Karman turbulence model was used for the turbulence model. The controller that we suggested showed during the longitudinal, lateral and hover flight that the isteccopter we developed has successfully controlled the dynamic models in both noise and noiseless environment.

References

- [1] A. Marks, J. F. Whidborne, and I. Yamamoto, "Control allocation for fault tolerant control of a VTOL octorotor," in *Control (CONTROL), 2012 UKACC International Conference on, 2012*, pp. 357-362.
- [2] G. Staples, "Propeller Static & Dynamic Thrust Calculation," ed, 2015.
- [3] S. Bouabdallah, P. Murrieri, and R. Siegwart, "Design and control of an indoor micro zankacopter," in *Robotics and Automation, 2004. Proceedings. ICRA'04. 2004 IEEE International Conference on, 2004*, pp. 4393-4398.
- [4] T. Oktay and S. Coban, "Simultaneous Longitudinal and Lateral Flight Control Systems Design for Both Passive and Active Morphing TUAVs," *Elektronika ir Elektrotechnika*, vol. 23, pp. 15-20, 2017.
- [5] Çoban, S , Oktay, T . (2018). Legal and Ethical Issues of Unmanned Aerial Vehicles. *Journal of Aviation*, 2 (1), 31-35. DOI: 10.30518/jav.421644
- [6] B. L. Stevens, F. L. Lewis, and E. N. Johnson, *Aircraft control and simulation: dynamics, controls design, and autonomous systems*: John Wiley & Sons, 2015.
- [7] Çoban, S . (2018). Variance Constrained Vibration Control of Morphing Tactical Unmanned Aerial Vehicles (TUAVs). *Avrupa Bilim ve Teknoloji Dergisi*, (14), 269-271. DOI: 10.31590/ejosat.475870
- [8] Çoban, S , Oktay, T . (2018). Simultaneous Design of a Small UAV (Unmanned Aerial Vehicle) Flight Control System and Lateral State Space Model. *Journal of Aviation*, 2 (2), 70-76. DOI: 10.30518/jav.461365
- [9] K. Alexis, G. Nikolakopoulos, and A. Tzes, "Constrained-control of a zankacopter helicopter for trajectory tracking under wind-gust disturbances," in *MELECON 2010-2010 15th IEEE Mediterranean Electrotechnical Conference, 2010*, pp. 1411-1416.
- [10] Oktay, T , Köse, O . (2019). Dynamic Modeling and Simulation of Quadcopter for Several Flight Conditions. *Avrupa Bilim ve Teknoloji Dergisi*, (15), 132-142. DOI: 10.31590/ejosat.507222